Journal of Power Sources 311 (2016) 144–152

Contents lists available at ScienceDirect

Journal of Power Sources

journal homepage: www.elsevier.com/locate/jpowsour

Electrochemically reduced graphene oxide/carbon nanotubes composites as binder-free supercapacitor electrodes

Qin Yang [a, *], Siu-Kwong Pang [b], Kam-Chuen Yung [a]

[a] Department of Industrial and System Engineering, The Hong Kong Polytechnic University, Hung Hom, Kowloon, Hong Kong
[b] Institute of Textiles and Clothing, Faculty of Applied Science and Textiles, The Hong Kong Polytechnic University, Hung Hom, Kowloon, Hong Kong

HIGHLIGHTS

- Binder-free electrodes were fabricated with MWCNTs and ecrGO for supercapacitors.
- MWCNTs as "spacers" insert between the graphene sheets to enlarge surface areas.
- GO can be reduced to ecrGO by a facile and controllable electrochemical method.
- The ecrGO/MWCNTs composite (GO:MWCNTs = 5:1) showed the highest C_{sp}.
- The composite (5:1) have high retention of 93% after 4000 charge/discharge cycles.

GRAPHICAL ABSTRACT

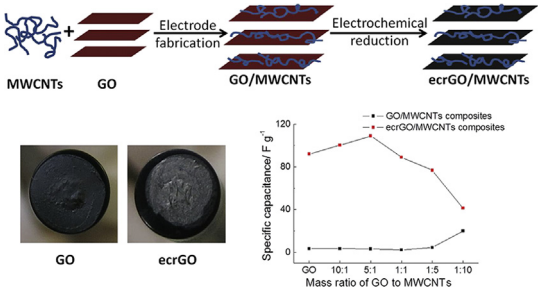

ARTICLE INFO

Article history:
Received 27 November 2015
Received in revised form
23 January 2016
Accepted 5 February 2016
Available online 18 February 2016

Keywords:
Graphene oxide
Reduced graphene oxide
Multiwalled carbon nanotubes
Electrochemical reduction
Binder-free electrodes
Supercapacitors

ABSTRACT

Binder-free composites of electrochemically reduced graphene oxide (ecrGO) and multiwalled carbon nanotubes (MWCNTs) were fabricated as supercapacitors electrodes operating in aqueous systems. GO was found to be electrochemically reduced according to the XRD and Raman data. Therefore, this facile and controllable method was applied to reduce GO in the GO/MWCNTs composites, generating ecrGO/MWCNTs composites. The ecrGO/MWCNTs composites exhibit higher specific capacitance (C_{sp}) than ecrGO because the intercalation of MWCNTs into ecrGO sheets increases the surface areas, according to the TEM, XRD and N_2 adsorption-desorption results. The composites with different mass ratios of GO to MWCNTs (10:1, 5:1, 1:1, 1:5, 1:10) were investigated. The ecrGO/MWCNTs composite (GO: MWCNTs = 5:1) showed the highest C_{sp} from the cyclic voltammetry results at a scan rate of 10 mV s^{-1}, and it expressed C_{sp} of 165 F g^{-1} at a current density of 1 A g^{-1} and 93% retention after 4000 cycles of charge/discharge. When the mass ratio of GO to MWCNTs further decreases to 1:10, the C_{sp} of the composites declines, and the ecrGO/MWCNTs composite (GO: MWCNTs = 1:10) performs a nearly pure double-layer capacitor. However, the composites containing more MWCNTs can maintain better capacitive behavior at higher rates of charge/discharge.

1. Introduction

Supercapacitors, as energy storage devices, involve two energy storage mechanisms: electric double layer capacitors (EDLCs) by

* Corresponding author.
E-mail address: qin.yang@connect.polyu.hk (Q. Yang).

http://dx.doi.org/10.1016/j.jpowsour.2016.02.016
0378-7753/

storing energy through the simple physical adsorption of ions, and pseudocapacitors by producing energy from redox reactions during charge/discharge [1,2]. Carbonaceous materials, such as carbon nanotubes, carbon fibers, graphene and activated carbon, have been widely investigated for the electrodes of supercapacitors [2–5], because they exhibit good conductivity, chemical stability and mechanical strength.

Multiwalled carbon nanotubes (MWCNTs) are considered as a promising electrode material for supercapacitors, due to the large surface area, good conductivity and high mechanical strength [4]. However, pristine MWCNTs have low capacitance (~38 F g^{-1} [6–8], varying with scan rates and types of electrolytes [8]), because only the electrostatic adsorption of ions contributes to the energy storage mechanism, and the hydrophobicity of MWCNTs also limits ions to accessing the electrode surfaces [9]. In order to overcome these limitations, functionalization of MWCNTs with strong thermal acids is widely used to improve their capacitance [10,11]. The capacitance of MWCNTs can also be improved by decorating with conducting polymers [12] or transition metals [13,14] which produce the pseudo-capacitance. In addition, some CNT based materials with 3D network structure have been developed [15,16] to improve the efficiency of ions accessing to the electrode surfaces, but these methods are time consuming and cumbersome to operate.

Theoretically, graphene can possess high double-layer capacitance due to its exceptional surface area (~2630 m^2 g^{-1}) [17]. However, the capacitance of graphene reported in experimental measurements is much lower than expected. This is because graphene sheets easily stack together, resulting in difficulty for the ions in permeating to the surface of graphene [18]. Therefore, some 3D structural materials have been developed using graphene or its composites with other carbon materials to facilitate the ion permeability to electrode surfaces [19–21].

In this study, GO as a graphene precursor and MWCNTs as "spacers" were used to fabricate binder-free electrodes, wherein the MWCNTs intercalate between the graphene sheets to avoid the graphene sheets stacking together. The reasons of the use of GO as a graphene precursor are as follows: First, GO can disperse homogeneously in water due to the hydrophilic groups, such as carboxyl and carbonyl groups on the surface of GO [22]. On the other hand, the basal plane of GO is hydrophobic [23], and contains π carbon bonds which can attract the π carbon bonds of MWCNTs through the π-π interaction [24]. GO, therefore, can serve as a surfactant to disperse MWCNTs in water to form GO/MWCNTs suspension in fabrication of electrodes. Second, GO can form a membrane after drying, thus no binder is necessary to fabricate electrodes.

GO has extremely poor conductivity (typical insulator, 10^{12} Ω sq^{-1} or higher [23]) because of the disruption of the sp^2-bonded carbon matrix by polar functional groups. To achieve better conductivity and higher capacitance, it is usually reduced to graphene. Therefore, electrochemical reduction [25,26] was used to reduce the GO in the GO/MWCNTs composites to form the electrochemically reduced GO (ecrGO) in the present study, producing the ecrGO/MWCNTs composites as binder-free electrodes. Compared with other reduction approaches such as chemical reduction [20,27] and thermal processing [19,21,28], the electrochemical reduction is more facile, low-cost and environmentally friendly. The schematic of the fabrication of the binder-free ecrGO/MWCNTs electrodes is shown in Fig. 1.

In this work, the capacitive and electrochemical performance of the composites was investigated in acids. Additionally, Raman spectroscopy, X-ray diffraction (XRD), Transmission electron microscopy (TEM) and the BET surface area analysis were used to characterize the composites of ecrGO/MWCNTs.

2. Experimental

2.1. GO/MWCNTs electrode fabrication

Multiwalled carbon nanotubes (length: 1–12 μm, outside diameter: 13–18 nm, purity: > 99 wt%) and graphene oxide (5 g L^{-1}, 79% carbon and 20% oxygen) were obtained from Cheap Tubes Inc., USA and Graphene-supermarket Inc., USA respectively. 5 g L^{-1} GO was diluted to 1 g L^{-1} with DI water and subjected to a 5-min ultrasonic process. The stable suspension of GO/MWCNTs were obtained by mixing 1 g L^{-1} GO and MWCNTs with different mass ratios (GO: MWCNTs = 1:0, 10:1, 5:1, 1:1, 1:5, 1:10) with 2-h ultrasonic treatment. A platinum plate, used as a current collector, was covered by suspension of GO/MWCNTs, and dried in an oven for 8 min at 150 °C to form the GO/MWCNTs binder-free electrodes. The mass loading of GO/MWCNTs composites on working electrode is around 1.8 mg cm^{-2}.

2.2. ecrGO/MWCNTs electrode preparation

The electrochemical reduction of GO/MWCNTs on electrodes was carried out with cyclic voltammetry (−1.2 V − 0 V) in a 0.5 M NaCl solution at a scan rate of 50 mV s^{-1}. A three-electrode system (platinum wire as a counter electrode and Ag/AgCl as a reference electrode), and a VersaSTAT potentiostat/galvanostat (Princeton Applied Research, USA) were employed.

2.3. Materials characterization

The morphology of the ecrGO/MWCNT composites was characterized by transmission electron microscopy (TEM, JEOL JEM-2010). The samples were dispersed in ethanol with 10 min of ultrasonic vibration. The dispersion was placed on a holey-carbon coated copper grid, and dried in an oven at 60 °C for 5 min. Raman spectra of the GO/MWCNTs composites and ecrGO/MWCNTs were recorded on a MicroRaman/Photoluminescence spectrometer (Renishaw InVia) equipped with a 633 nm Ar ion laser. The phase structures of the composites and their constituents were characterized by an X-ray diffraction (XRD) system (PANalytical), ranging from 5° to 50° at a scan rate of 5° min^{-1}. The nitrogen adsorption/desorption isothermal curves of the composites were obtained using an Autosorb instrument (Quantachrome Instruments) at 77 K, and the surface areas were calculated based on the Brunauer-Emmett-Teller (BET) method.

2.4. Electrochemical measurements

The electrochemical performance of the electrodes was measured in 1 M HCl by a VersaSTAT potentiostat/galvanostat (Princeton Applied Research, USA), using a pure Pt wire and Ag/AgCl as a counter electrode and a reference electrode respectively. The electrochemical techniques employed in this study included cyclic voltammetry (CV), chronopotentiometry (charge and discharge at constant currents) and electrochemical impedance spectroscopy (EIS). The EIS was applied in a frequency range from 100 kHz to 0.1 Hz using a dc voltage of 0.4 V (the middle voltage of the operating potential window 0 V − 0.8 V), superimposed with an ac amplitude of 5 mV.

3. Results and discussion

3.1. Formation of ecrGO by electrochemical reduction of GO

GO films were immersed in 0.5 M NaCl and electrochemically reduced to ecrGO films by cycling between −1.2 V and 0 V at a scan

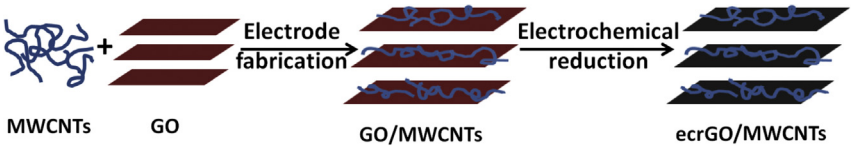

Fig. 1. Schematic of fabrication of binder-free ecrGO/MWCNTs electrodes.

rate of 50 mV s^{-1}, as shown in the CV curves of Fig. 2a. The GO films are dark brown, whereas the ecrGO films has a grey metal luster, so the results indicate the efficient reduction of GO to ecrGO [29]. As shown in the CV curves in Fig. 2a, the current increases with the number of CV cycles because more conductive ecrGO is formed from non-conductive GO [26].

Fig. 2b shows the CV behavior of ecrGO films in 1 M HCl at a scan rate of 10 mV s^{-1} between 0 V and 0.8 V, after different numbers of electrochemical reduction cycles for GO. Pairs of redox peaks appear around +0.4 V, corresponding to the redox reactions of ecrGO. The specific capacitance can be calculated based on the CV curves according to the following equation [5,30],

$$C_{sp} = \frac{1}{mv(V_2 - V_1)} \int_{V_1}^{V_2} I(V)dV \quad (1)$$

where C_{sp} is the specific capacitance (F g^{-1}), m is the mass of composites, v is the potential scan rate (V s^{-1}), V_1 and V_2 are the switching potential in cyclic voltammetry (V), and $I(V)$ denotes the response current (A), $\int_{V_1}^{V_2} I(V)dV$ is voltammetric charge obtained by integration of positive or negative sweep in cyclic voltammograms [30]. Here, the specific capacitance is obtained by averaging the voltammetric charge of positive and negative sweep, according to the equation (2).

$$C_{sp} = \frac{C_{sp(\text{positive sweep})} + C_{sp(\text{negative sweep})}}{2} \quad (2)$$

As shown in Fig. 2c, the C_{sp} of GO is ~5 F g^{-1}, and that of ecrGO can achieve ~88 F g^{-1} after 90 cycles of electrochemical reduction of GO, indicating that GO has poor capacitive performance relative to ecrGO. The C_{sp} increases with the number of electrochemical reduction cycles for GO, and begin to get stable after 70 electrochemical reduction cycles (Fig. 2c). In the later electrochemical evaluation, the composites of GO/MWCNTs were reduced to ecrGO/MWCNTs composites by 70 electrochemical reduction cycles. There are three advantages in employing the ecrGO as electrodes for supercapacitors: (i) the preparation of ecrGO is easily operated through adjusting the number of CV cycles; (ii) the pseudocapacitance from ecrGO can contribute to the overall capacitance; (iii) no binders (PTFE or carbon black) are necessary because they may affect the properties of the electrodes.

3.2. Structural characterization

Structural characterization of GO, MWCNTs and the composite of GO/MWCNTs were conducted, and the ecrGO/MWCNTs composite with the mass ratio of GO:MWCNTs = 5:1 was selected because the ecrGO/MWCNTs composite (GO:MWCNTs = 5:1) exhibits the highest specific capacitance at the scan rate of 10 mV s^{-1}, when comparing with the ecrGO/MWCNTs composites with other mass ratios. The electrochemical performance of the ecrGO/MWCNTs composites with different mass ratios will be discussed in detail in the Section 3.3.

Fig. 3a, b and c show the TEM images of the structures of ecrGO, the ecrGO/MWCNTs composite with a mass ratio of GO: MWCNTs = 5:1 and MWCNTs respectively, with a measuring scale of 200 nm. It can be clearly seen that the ecrGO is a continuous film with wrinkles at this scale (Fig. 3a), and the MWCNTs, as indicated by the black arrows, scatter well throughout the ecrGO sheets in the ecrGO/MWCNTs composite (Fig. 3b). The MWCNTs alone prefer to agglomerate (Fig. 3c). Therefore, GO can serve as a surfactant to disperse MWCNTs in water to form GO/MWCNTs suspension in fabrication of electrodes. From Fig. 3b, MWCNTs can intercalate between the ecrGO sheets to form a sandwich-like structure which results in exposing more surface areas of ecrGO in the ecrGO/MWCNTs composites.

The Raman spectra of GO and ecrGO are depicted in Fig. 4a. Two main peaks of the band D (~1340 cm^{-1}) corresponding to the structural defects [31], and the band G (~1560 cm^{-1}) denoting the in-plane vibration of sp^2 carbon atoms [32], can be observed in Fig. 4a. The ratio of I_D: I_G for GO is 1.06, and then it increases to 1.58 for ecrGO. When comparing with GO, the increased I_D: I_G ratio for ecrGO demonstrates the formation of structural defects [31,33] after electrochemical reduction of GO. The MWCNTs exhibit the highest ratio of I_D: I_G (2.06), then its ratio of I_D: I_G decreases to 1.21 after mixing with GO to fabricate the GO/MWCNTs composite (GO: MWCNTs = 5:1). It is attributed that more sp^2 carbon atoms from GO make the G peak higher. When GO/MWCNTs are electrochemically reduced to ecrGO/MWCNTs, the ratio of I_D: I_G increases from 1.21 to 1.33 due to the structural defects from ecrGO.

Fig. 4b shows the XRD patterns of GO, ecrGO, GO/MWCNTs (mass ratio of GO: MWCNTs = 5:1), ecrGO/MWCNTs (mass ratio of GO: MWCNTs = 5:1) and MWCNTs. A diffraction peak of MWCNTs at 25.9° was observed, reflecting the characteristic of graphite [34]. Sharp peaks for GO alone and GO in the GO/MWCNTs composite appear around 10°, while the XRD angle for the GO/MWCNTs (10.12°) is slightly smaller than GO (10.4°) as shown in Fig. 4b insert, indicating the larger distance between GO sheets in the GO/MWCNTs composite than the GO alone, and it may be attributed to the MWCNTs intercalating between GO sheets. These peaks disappear for ecrGO and are replaced by a broad peak around 24.5° for ecrGO alone and ecrGO in the ecrGO/MWCNTs composite. It is attributed that the spatial arrangement of the GO sheets is different from that of ecrGO sheets. The GO/MWCNTs composites also express a broad peak at around 24.5°, and it implies that the intercalation of MWCNTs changes the spatial arrangement of the GO sheets.

To further confirm the higher surface area of the ecrGO/MWCNTs composites compared to the ecrGO, the BET surface areas of them were obtained using the nitrogen adsorption-desorption isothermal curves shown in Fig. 4c. It is a type I curve at low relative pressure (0.01–0.4), then a hysteresis loop appears at high relative pressure from 0.4 to 1, indicating the existence of microporosity, mesoporosity and macroporosity [35]. The BET surface area of GO was 362 m^2 g^{-1} after fabricating the electrode. After electrochemical reduction, the surface area of ecrGO was 50.7 m^2 g^{-1}, lower than the surface area of GO (362 m^2 g^{-1}). It may be attributed to the removal of the functional groups isolated on the GO sheets, leading to the ecrGO sheets to stack together more closely. When the MWCNTs intercalate between the GO sheets, the

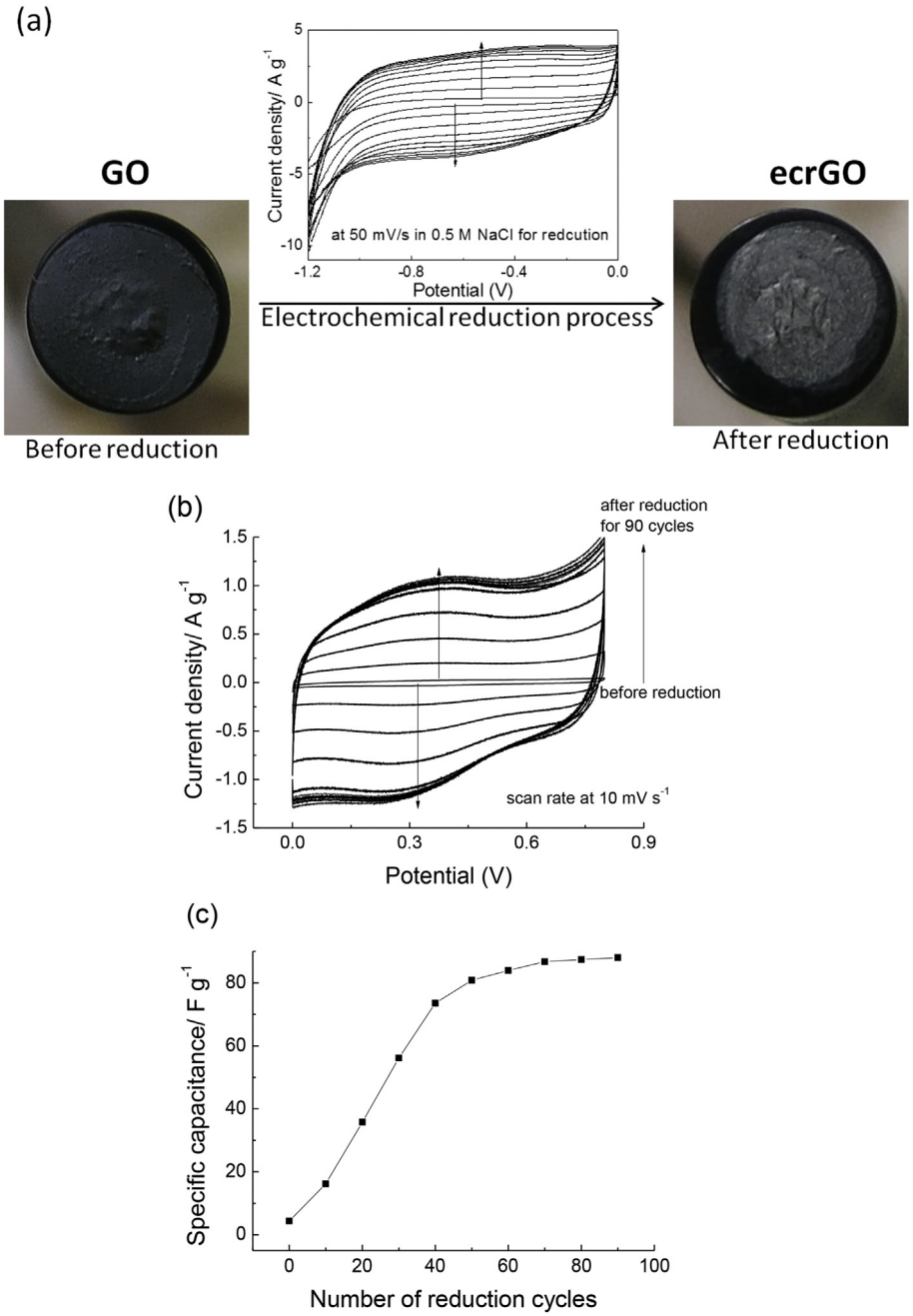

Fig. 2. (a) Electrochemical reduction of GO in 0.5 M NaCl at a scan rate of 50 mV s^{-1}, obtained using an Ag/AgCl reference electrode, and images of GO (left) and ecrGO (right). (b) Cyclic voltammograms of ecrGO films in 1 M HCl at a scan rate of 10 mV s^{-1} after various CV cycles for electrochemical reduction of GO, obtained using an Ag/AgCl reference electrode. (c) The specific capacitance of ecrGO as a function of the number of electrochemical reduction cycles for GO.

measured surface area of the ecrGO/MWCNTs composite (GO: MWCNT = 5:1) is 113.5 m^2 g^{-1}, which is two times higher than the surface area of ecrGO (50.7 m^2 g^{-1}). The results demonstrate that the intercalation of MWCNTs between ecrGO sheets can expose more surface areas of ecrGO in the ecrGO/MWCNTs composites, resulting in uplifting the capacitive performance. Although the isothermal curve for MWCNTs indicates that MWCNTs have greater surface area (224 m^2 g^{-1}) than ecrGO (50.7 m^2 g^{-1}), the proportion of the MWCNTs in the ecrGO/MWCNTs composite (GO: MWCNT = 5:1) is small (one sixth of the composite mass), so MWCNTs themselves in proportion cannot significantly contribute to the two-fold increase in the surface area.

3.3. Electrochemical performance of ecrGO/MWCNTs composites

The cyclic voltammograms of ecrGO/MWCNTs composites with different mass ratios (GO: MWCNTs = 1:0; 10:1; 5:1; 1:1; 1:5; 1:10) are shown in Fig. 5a. When comparing with GO (Fig. 5a, black line), the CV curve of ecrGO shows much larger current density (Fig. 5a, red line). This is attributed to the much higher conductivity of ecrGO than GO. There are broad redox peaks around +0.4 V for the ecrGO/MWCNTs composites with the higher ecrGO content (GO: MWCNTs = 1:1 or above), indicating the existence of a faradic process in ecrGO. The broad peaks may be generated by a multi-step faradic process that several redox peaks overlap with one

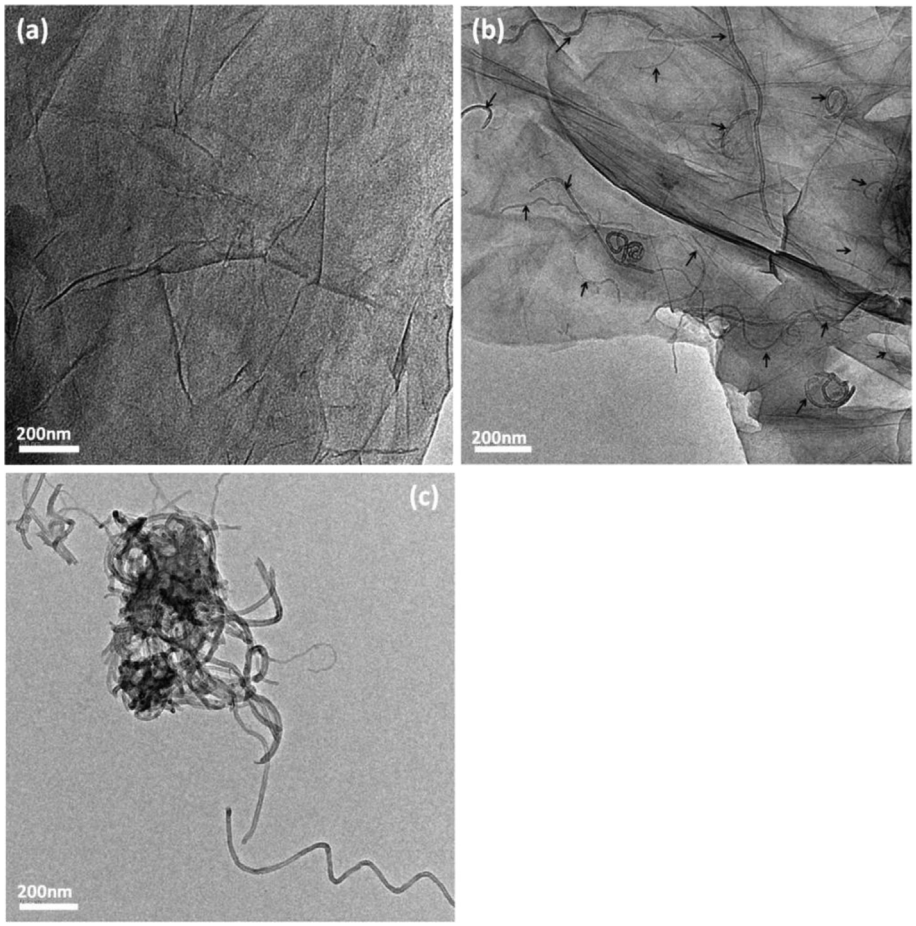

Fig. 3. TEM images of structures of (a) ecrGO; (b) ecrGO/MWCNTs composite with a mass ratio of GO: MWCNTs = 5:1; (c) MWCNTs.

another according to the CV curves for the composites with the lower ecrGO content (GO: MWCNTs = 1:5 or below) in Fig. 5a. Fig. 5b shows the specific capacitance of ecrGO/MWCNTs composites with different mass ratios of GO to MWCNTs as a function of the number of CV cycles. The C_{sp} of the composites become stable after 300 CV cycles. Fig. 5c depicts the specific capacitance of the ecrGO/MWCNTs composites with various mass ratios of GO to MWCNTs (all the C_{sp} values in Fig. 5c were calculated based on the corresponding 300^{th} CV cycle). The C_{sp} of ecrGO is ~90 F g^{-1}. When the mass ratio of GO to MWCNTs decreases from 10:1 to 5:1, the C_{sp} of the ecrGO/MWCNTs composites elevates to the highest value (~110 F g^{-1}). However, the C_{sp} of the composites declines to 88 F g^{-1}, 76 F g^{-1} and 41 F g^{-1} when the ratio further decreases to 1:1, 1:5 and 1:10 respectively. Theoretically, ecrGO/MWCNTs composites containing more MWCNTs may display lower specific capacitance because carbon nanotubes have smaller specific capacitance than graphene [31,36]; however, there is an optimum mass ratio of GO to MWCNTs (5:1). It can be attributed to the higher specific surface area of ecrGO/MWCNTs (GO: MWCNTs = 5:1) compared to ecrGO. MWCNTs, here, act as "spacers" between the graphene sheets to prevent the sheets from stacking together, thus enlarging the specific surface areas of electrode materials. When the content of MWCNTs in the composites increases further, the MWCNTs dominate the capacitive performance of ecrGO/MWCNTs composites, causing the decrease in specific capacitance.

The capacitive performance of the composites with different mass ratios of GO to MWCNTs at a scan rate of 10 mV s^{-1} and other scan rates (50 mV s^{-1}, 100 mV s^{-1}, 200 mV s^{-1}, 400 mV s^{-1}) in 1 M HCl are shown in Fig. 5a and Fig. 6a–d respectively. Under 100 mV s^{-1}, all the ecr/MWCNTs composites can more or less maintain the quasi-rectangular shape of the CV curves, but not ecrGO at 50 mV s^{-1} and 100 mV s^{-1} (Fig. 6a and b). The ecrGO/MWCNTs composites with the mass ratios of GO to MWCNTs equal to 10:1 at 200 mV s^{-1} (Fig. 6c), and 5:1 at 400 mV s^{-1} (Fig. 6d) lose the quasi-rectangular shape of the CV curves. (Fig. 6d). The results indicate that the composites containing more ecrGO are difficult to resist the distortion of the quasi-rectangular shape of the CV curves at high scan rates.

In addition, Fig. 6e shows that the specific capacitance of the ecrGO/MWCNTs composites containing more ecrGO (GO: MWCNTs = 1:0, 10:1, 5:1) decreases more rapidly with increasing the scan rate when comparing with the composites with less ecrGO (GO: MWCNTs = 1:1, 1:5 and 1:10). The distortion of the CV curves and the greater drop of specific capacitance of the composites with more ecrGO at high scan rates may be caused by the ion-diffusion limitation, because the resistance of ion permeability to the electrode surfaces increases when more ecrGO sheets stack together. This ion-diffusion limitation will be revealed by the EIS data (Fig. 7) later. Moreover, there are crossovers in Fig. 6e that the specific capacitance of the composites with more MWCNTs (GO: MWCNTs = 1:1 and 1:5) become the greatest at the highest scan rate (400 mV s^{-1}). Therefore, it is proposed that those composites with more MWCNTs can be used in the application of high charge/discharge rates.

The electrochemical impedance spectroscopy (EIS) was measured from 100 kHz to 0.1 Hz, at 0.4 V dc superimposed with an

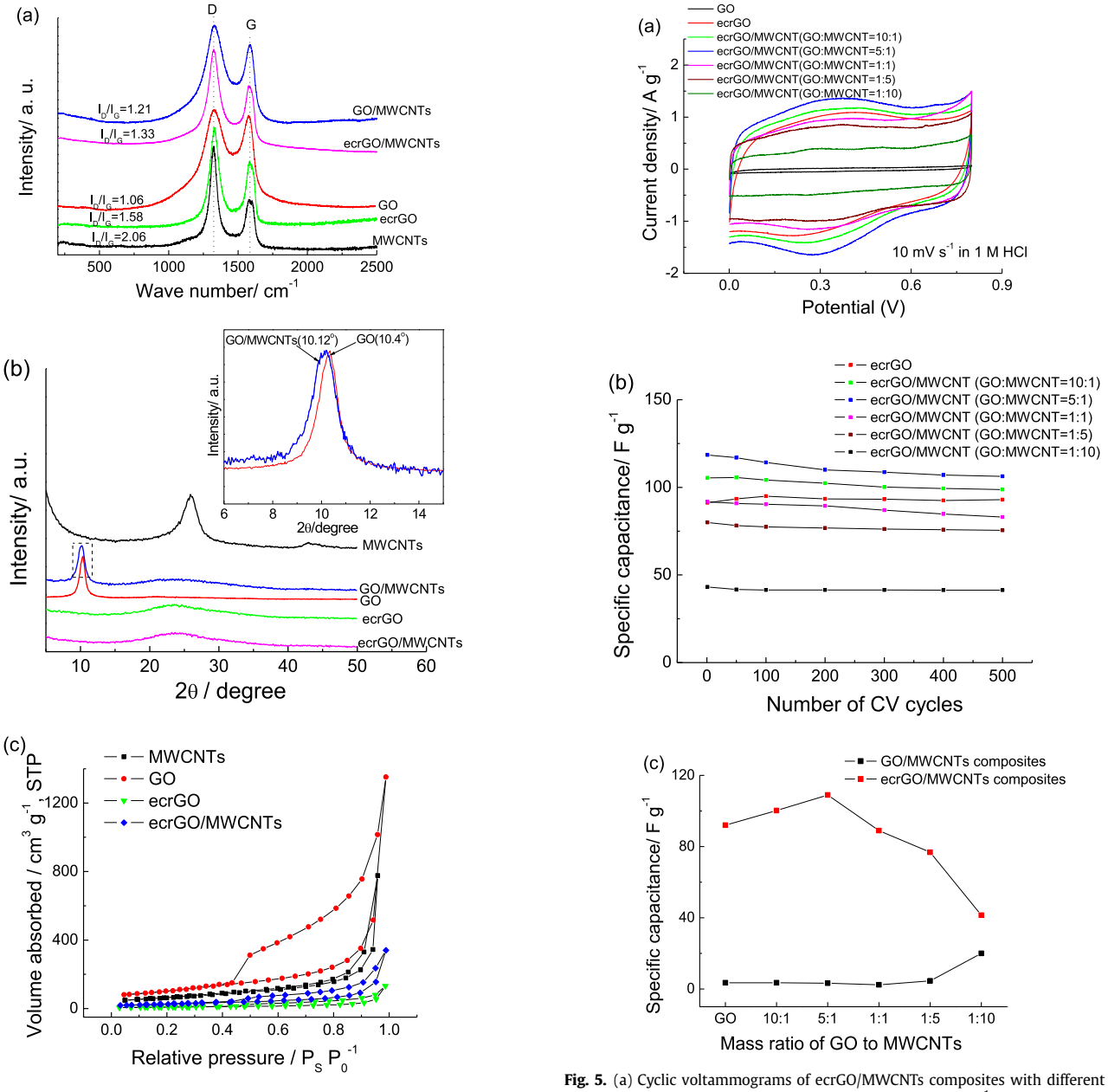

Fig. 4. (a) Raman spectra and (b) XRD patterns of MWCNTs, GO, ecrGO, GO/MWCNTs composite (GO: MWCNTs = 5:1) and ecrGO/MWCNTs composite (GO: MWCNTs = 5:1). (c) Nitrogen adsorption-desorption isothermal curves of GO, ecrGO, MWCNTs and ecrGO/MWCNTs composite (GO: MWCNT = 5:1).

Fig. 5. (a) Cyclic voltammograms of ecrGO/MWCNTs composites with different mass ratios of GO to MWCNTs in 1 M HCl at a scan rate of 10 mV s^{-1}, obtained using an Ag/AgCl electrode. (b) Cyclability of ecrGO and ecrGO/MWCNTs composites. (c) Specific capacitance of GO/MWCNTs composites and ecrGO/MWCNTs composites at the 300th CV cycle as a function of the mass ratio of GO to MWCNTs.

ac amplitude of 5 mV. Nyquist plots of the ecrGO/MWCNTs composites with different mass ratios of GO to MWCNTs are depicted in Fig. 7a. The semicircles in the high-frequency range (the insert in Fig. 7a) and the inclined lines in the low-frequency range (Fig. 7a) correspond to the charge transfer resistance (R_{ct}) regarding the faradic process in ecrGO and the diffusion-controlled process respectively [37]. The higher inclination of the lines from the vertical in the low-frequency region reflects the greater resistance of the ion permeability to electrode surfaces [38] because more ecrGO sheets stack together. Therefore, the slopes of the lines in the low-frequency region become more vertical when the content of ecrGO decreases, indicating that composites containing more MWCNTs (less ecrGO) exhibit a more ideal double-layer capacitor. These EIS results cohere with the CV data that the composites containing more MWCNTs can maintain their capacitive performance (the quasi-rectangular shape of CV curves in Fig. 6) at higher scan rates. The distorted semicircles in the high frequency region become the quasi-semicircles when the ecrGO content in the composites decreases. These results reflect that the intercalation of MWCNTs between ecrGO sheets can affect the mechanism of the faradic process in ecrGO.

Fig. 7b shows the imaginary part of the specific capacitance as a function of frequency. The relaxation time constant τ_0 is a characteristic of the capacitive system: the minimum time required for discharge with efficiency greater than 50% of its maximum value. It can be obtained through $\tau_0 = (2\pi f_0)^{-1}$ where f_0 is the value at which the imaginary capacitance C″ is maximum [39,40]. The ecrGO/MWCNTs (GO: MWCNTs = 1:10) composite exhibits the

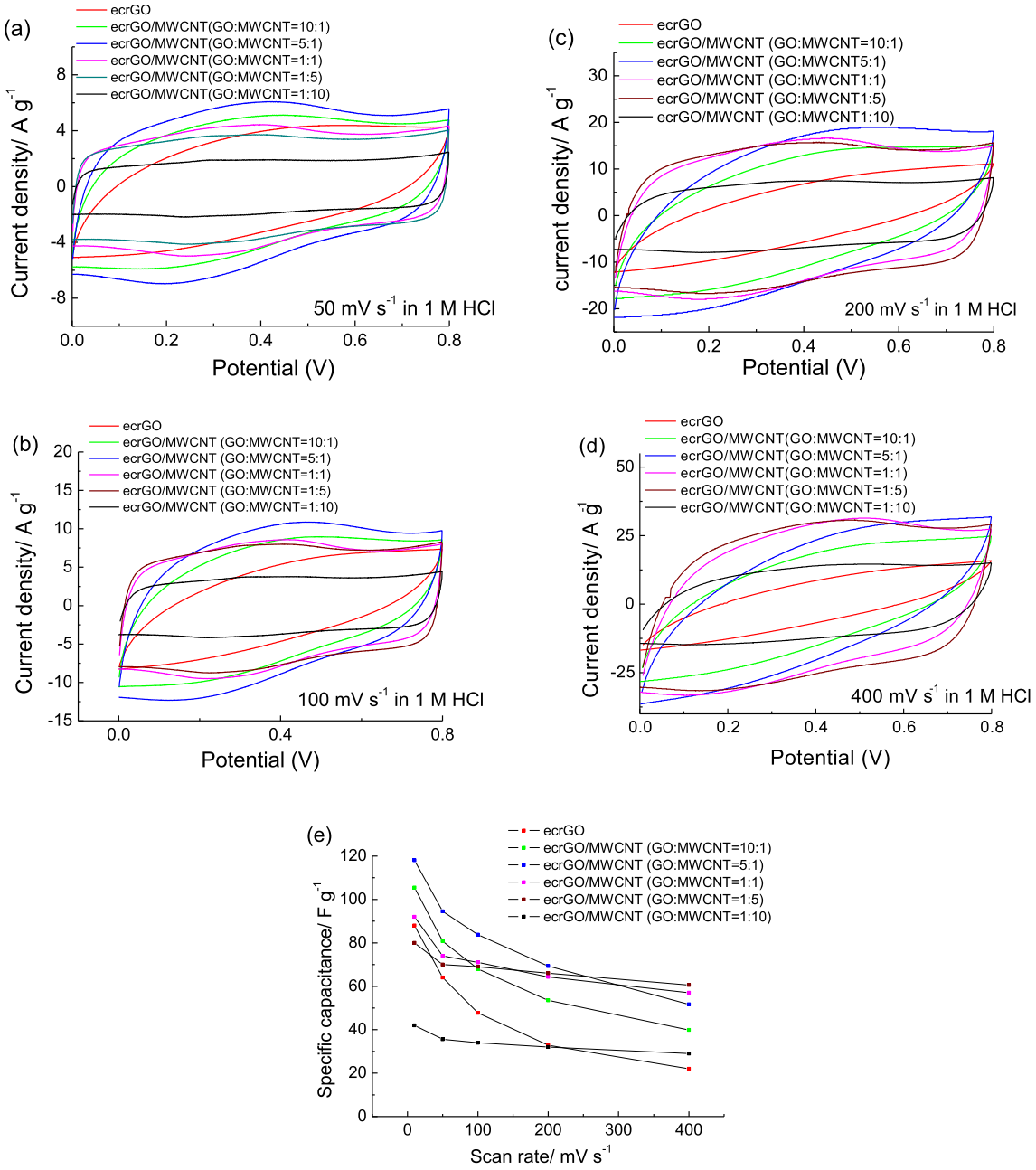

Fig. 6. Cyclic voltammograms of the ecrGO/MWCNTs composites with different mass ratios of GO: MWCNT (1:0, 10:1, 5:1, 1:1, 1:5, 1:10) at diverse scan rates: (a) 50 mV s^{-1}; (b) 100 mV s^{-1}; (c) 200 mV s^{-1}; (d) 400 mV s^{-1} in 1 M HCl solutions, obtained using an Ag/AgCl reference electrode. (e) The specific capacitance of the ecrGO/MWCNTs composites with different mass ratios (1:0, 10:1, 5:1, 1:1, 1:5, 1:10) at various scan rates (10 mV s^{-1}, 50 mV s^{-1}, 100 mV s^{-1}, 200 mV s^{-1}, 400 mV s^{-1}).

shortest time constant of 0.1 s, and the relaxation time constant τ_0 increases to 0.16 s, 0.25 s and 1.27 s when the mass ratio of GO: MWCNTs increases to 1:5, 1:1 and 5:1 correspondingly. It indicates that ecrGO/MWCNTs composites containing more MWCNTs (shorter time constant) can behave like double-layer capacitors at higher rates of charge and discharge. These results align with the data of the scan rate-dependent CV curves (Fig. 6), that composites containing more MWCNTs can maintain a quasi-rectangular CV curve at higher scan rates.

The galvanostatic charge/discharge curves of the ecrGO/MWCNTs composite (GO: MWCNTs = 5:1) at current densities (1 A g^{-1}, 2 A g^{-1}, 4 A g^{-1}) are plotted in Fig. 8a. All these curves exhibit a triangular shape with little distortion, implying a good capacitive behavior for the composite. According to equation (3), the specific capacitance of the ecrGO/MWCNTs composite (GO: MWCNTs = 5:1) at different constant current densities were obtained.

$$C_{sp} = \frac{I\,\Delta t}{m(V_2 - V_1)} \tag{3}$$

where I/m is the constant current density for discharge, Δt is the time of discharge, V_2 and V_1 are the initial and final potentials for discharge.

4000 cycles of charge/discharge of the ecrGO/MWCNTs composite (GO: MWCNTs = 5:1) were measured (Fig. 8b). The C_{sp} of the composite was 177 F g^{-1} (98.9% of the initial value) at a current

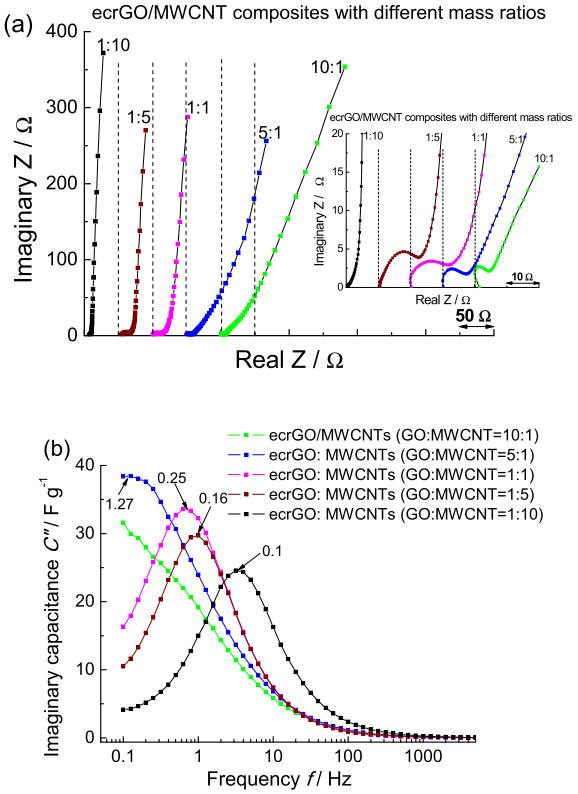

Fig. 7. (a) Nyquist plots of ecrGO/MWCNTs composites with different mass ratios of GO: MWCNTs (10:1, 5:1, 1:1, 1:5, 1:10), at 5 mV (ac) superimposed on 0.4 V (dc) vs. Ag/AgCl with frequencies ranged from 100 kHz to 0.1 Hz, measured in 1 M HCl solutions; (b) imaginary part of capacitance (C″) as a function of frequency.

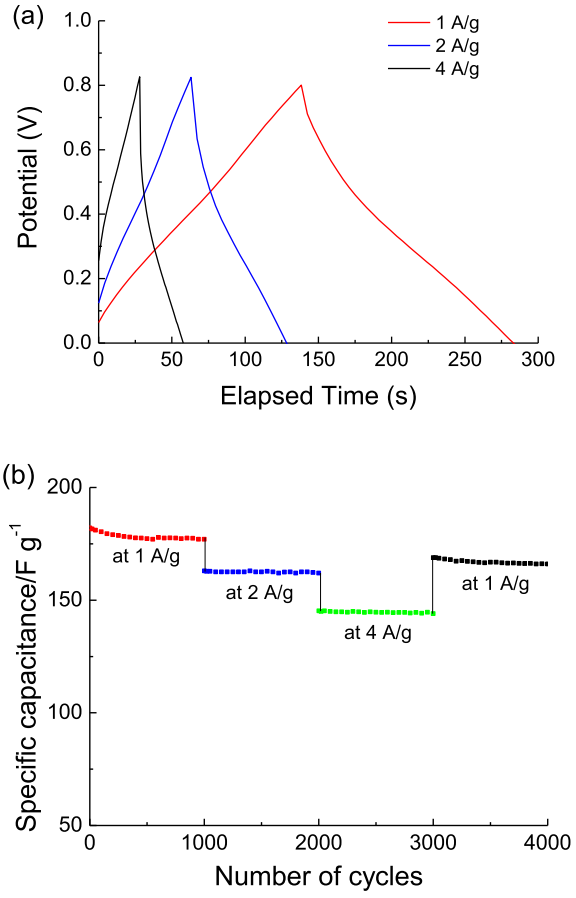

Fig. 8. (a) Galvanostatic charge/discharge for the ecrGO/MWCNTs composites (GO: MWCNTs = 5:1) at current densities of 1 A g^{-1}, 2 A g^{-1}, 4 A g^{-1}; (b) Cycling performance of the ecrGO/MWCNTs composite (GO: MWCNTs = 5:1) at varying current densities.

density of 1 A g^{-1} after 1000 cycles of charge/discharge. C_{sp} of 162 F g^{-1} (~10% drop) at 2 A g^{-1} and 145 F g^{-1} (~20% drop) at 4 A g^{-1} were obtained at the 2000th cycle and the 3000th cycle respectively. C_{sp} of 165 F g^{-1} was measured at the 4000th cycle when returning to a current density of 1 A g^{-1}, and retention of 93% could be achieved.

Combined analysis of the CV and BET data reveals that the surface areas of the materials do not always dominate the specific capacitance. This is because when the MWCNT content in the ecrGO/MWCNTs composites increases beyond the optimum point, the specific capacitance lowers instead (Fig. 5c) although MWCNTs (224 m^2 g^{-1}) have a larger surface area than ecrGO (50.7 m^2 g^{-1}). Furthermore, even though the surface area of GO (362 m^2 g^{-1}) is greater than that of ecrGO (50.7 m^2 g^{-1}), the specific capacitance of GO is much smaller than ecrGO (Fig. 5a). Therefore, the specific capacitance of the ecrGO/MWCNTs composites can be the interplay of the faradic process in ecrGO, the polar functional groups left in ecrGO due to incomplete electrochemical reduction, and the conductivity and the surface areas of the materials.

4. Conclusions

ecrGO/MWCNTs composites were fabricated as binder-free electrodes for supercapacitors. A facile and controllable electrochemical reduction method was applied to convert the GO to ecrGO. MWCNTs can act as “spacers” intercalating into GO sheets to enlarge the surface area of composites, hence increase the C_{sp} of the ecrGO/MWCNTs composites. However, there is an optimum MWCNT content, and beyond the optimum value, the C_{sp} of the ecrGO/MWCNTs composites decreases. It is attributed to the smaller pseudo-capacitance due to the lower ecrGO content in the composites. Furthermore, at higher scan rates, the composites containing more MWCNTs (less ecrGO), can behave more like a double-layer capacitor, maintain a better capacitive behavior, and resist a drop of C_{sp} better; and hence the optimum MWCNTs content in the composite will change with the scan rate. This is because the stacking of the ecrGO sheets limits the ion-diffusion in the composites. Therefore, more MWCNTs in ecrGO/MWCNTs composites are proposed to be used in the application of higher rate of charge and discharge. Also, it was found that the surface areas did not always play a major role in the design of the supercapacitor electrodes from the combined analysis of the CV and BET data, and the faradic process in ecrGO, the polar functional groups left in ecrGO due to incomplete electrochemical reduction, and the conductivity of the materials should be taken into consideration.

Acknowledgements

The work described in this paper was supported by the Research Committee of The Hong Kong Polytechnic University under project No.RTAP. Technical assistance from the Department of Chemical and Biomolecular Engineering (CBME) of Hong Kong University of Science and Technology (HKUST) is appreciated.

References

[1] C. Liu, Z. Yu, D. Neff, A. Zhamu, B.Z. Jang, Nano Lett. 10 (2010) 4863–4868.
[2] G. Wang, L. Zhang, J. Zhang, Chem. Soc. Rev. 41 (2012) 797–828.

[3] C. Portet, P.L. Taberna, P. Simon, E. Flahaut, C. Laberty-Robert, Electrochimica Acta 50 (2005) 4174–4181.
[4] L.L. Zhang, X.S. Zhao, Chem. Soc. Rev. 38 (2009) 2520–2531.
[5] Q. Yang, S.-K. Pang, K.-C. Yung, J. Electroanal. Chem. 728 (2014) 140–147.
[6] Z. Niu, W. Zhou, J. Chen, G. Feng, H. Li, W. Ma, J. Li, H. Dong, Y. Ren, D. Zhao, S. Xie, Energy & Environ. Sci. 4 (2011) 1440–1446.
[7] X. Zhao, B.T.T. Chu, B. Ballesteros, W. Wang, C. Johnston, J.M. Sykes, P.S. Grant, Nanotechnology 20 (2009).
[8] S. Bose, T. Kuila, A.K. Mishra, R. Rajasekar, N.H. Kim, J.H. Lee, J. Mater. Chem. 22 (2012) 767–784.
[9] S.H. Aboutalebi, A.T. Chidembo, M. Salari, K. Konstantinov, D. Wexler, H.K. Liu, S.X. Dou, Energy & Environ. Sci. 4 (2011) 1855–1865.
[10] Y. Shao, G. Yin, J. Zhang, Y. Gao, Electrochimica Acta 51 (2006) 5853–5857.
[11] J. Shen, A. Liu, Y. Tu, G. Foo, C. Yeo, M.B. Chan-Park, R. Jiang, Y. Chen, Energy & Environ. Sci. 4 (2011) 4220–4229.
[12] Q. Yang, S.-K. Pang, K.-C. Yung, J. Electroanal. Chem. 758 (2015) 125–134.
[13] Q. Xiao, X. Zhou, Electrochimica Acta 48 (2003) 575–580.
[14] R.A. Fisher, M.R. Watt, W. Jud Ready, ECS J. Solid State Sci. Technol. 2 (2013) M3170–M3177.
[15] S. He, L. Chen, C. Xie, H. Hu, S. Chen, M. Hanif, H. Hou, J. Power Sources 243 (2013) 880–886.
[16] S. He, H. Hou, W. Chen, J. Power Sources 280 (2015) 678–686.
[17] Q. Cheng, J. Tang, J. Ma, H. Zhang, N. Shinya, L.-C. Qin, Phys. Chem. Chem. Phys. 13 (2011) 17615–17624.
[18] N. Jung, S. Kwon, D. Lee, D.-M. Yoon, Y.M. Park, A. Benayad, J.-Y. Choi, J.S. Park, Adv. Mater. 25 (2013) 6854–6858.
[19] D.T. Pham, T.H. Lee, D.H. Luong, F. Yao, A. Ghosh, V.T. Le, T.H. Kim, B. Li, J. Chang, Y.H. Lee, ACS Nano 9 (2015) 2018–2027.
[20] H. Fei, C. Yang, H. Bao, G. Wang, J. Power Sources 266 (2014) 488–495.
[21] Y. Yoon, K. Lee, S. Kwon, S. Seo, H. Yoo, S. Kim, Y. Shin, Y. Park, D. Kim, J.-Y. Choi, H. Lee, ACS Nano 8 (2014) 4580–4590.
[22] C. Petit, M. Seredych, T.J. Bandosz, J. Mater. Chem. 19 (2009) 9176–9185.
[23] S. Pei, H.-M. Cheng, Carbon 50 (2012) 3210–3228.
[24] C. Wu, X. Huang, X. Wu, L. Xie, K. Yang, P. Jiang, Nanoscale 5 (2013) 3847–3855.
[25] M. Zhou, Y. Wang, Y. Zhai, J. Zhai, W. Ren, F. Wang, S. Dong, Chem. – A Eur. J. 15 (2009) 6116–6120.
[26] Y. Shao, J. Wang, M. Engelhard, C. Wang, Y. Lin, J. Mater. Chem. 20 (2010) 743–748.
[27] C.K. Chua, M. Pumera, Chem. Soc. Rev. 43 (2014) 291–312.
[28] B. Zhao, P. Liu, Y. Jiang, D. Pan, H. Tao, J. Song, T. Fang, W. Xu, J. Power Sources 198 (2012) 423–427.
[29] C. Liu, F. Hao, X. Zhao, Q. Zhao, S. Luo, H. Lin, Sci. Rep. 4 (2014).
[30] H. Li, J. Wang, Q. Chu, Z. Wang, F. Zhang, S. Wang, J. Power Sources 190 (2009) 578–586.
[31] G.T.S. How, A. Pandikumar, H.N. Ming, L.H. Ngee, Sci. Rep. 4 (2014).
[32] K. Ai, Y. Liu, L. Lu, X. Cheng, L. Huo, J. Mater. Chem. 21 (2011) 3365–3370.
[33] Z. Ji, X. Shen, M. Li, H. Zhou, G. Zhu, K. Chen, Nanotechnology 24 (2013) 115603.
[34] H. Xia, Y. Wang, J. Lin, L. Lu, Nanoscale Res. Lett. 7 (2012) 1–10.
[35] G. Srinivas, Y. Zhu, R. Piner, N. Skipper, M. Ellerby, R. Ruoff, Carbon 48 (2010) 630–635.
[36] M.E. Birch, T.A. Ruda-Eberenz, M. Chai, R. Andrews, R.L. Hatfield, Ann. Occup. Hyg. 57 (9) (2013) 1148–1166.
[37] J. Yang, S. Gunasekaran, Carbon 51 (2013) 36–44.
[38] R. Farma, M. Deraman, Awitdrus, I.A. Talib, R. Omar, J.G. Manjunatha, M.M. Ishak, N.H. Basri, B.N.M. Dolah, Int. J. Electrochem. Sci. 8 (2013) 257–273.
[39] H. Kurig, A. Jänes, E. Lust, J. Electrochem. Soc. 157 (2010) A272–A279.
[40] K. Sheng, Y. Sun, C. Li, W. Yuan, G. Shi, Sci. Rep. 2 (2012) 247.